

Synthesis, Structure, and Molecular Orbital Studies of Yttrium, Erbium, and Lutetium Complexes Bearing η^2 -Pyrazolato Ligands: Development of a New Class of Precursors for Doping Semiconductors

Dirk Pfeiffer,^{1a} Bhekumusa J. Ximba,^{1a} Louise M. Liable-Sands,^{1b} Arnold L. Rheingold,^{1b} Mary Jane Heeg,^{1a} David M. Coleman,^{1a} H. Bernhard Schlegel,^{1a} Thomas F. Kuech,^{1c} and Charles H. Winter*,^{1a}

Department of Chemistry, Wayne State University, Detroit, Michigan 48202, Department of Chemistry, University of Delaware, Newark, Delaware 19716, and Department of Chemical Engineering, University of Wisconsin, Madison, Wisconsin 53706

Received March 23, 1999

Treatment of yttrium metal with bis(pentafluorophenyl)mercury (1.5 equiv), 3,5-di-*tert*-butylpyrazole (3 equiv), and pyridine (2 equiv) in toluene at ambient temperature for 120 h afforded tris(3,5-di-*tert*-butylpyrazolato)bis(pyridine)yttrium(III) (33%). In an analogous procedure, the reaction of erbium metal with 3,5-dialkylpyrazole (alkyl = methyl or *tert*-butyl), bis(pentafluorophenyl)mercury, and a neutral nitrogen donor (4-*tert*-butylpyridine, pyridine, *n*-butylimidazole, or 3,5-di-*tert*-butylpyrazole) yielded tris(3,5-di-*tert*-butylpyrazolato)bis(4-*tert*-butylpyridine)erbium(III) (63%), tris(3,5-di-*tert*-butylpyrazolato)bis(pyridine)erbium(III) (88%), tris(3,5-di-*tert*-butylpyrazolato)bis(*n*-butylimidazole)erbium(III) (48%), tris(3,5-dimethylpyrazolato)bis(4-*tert*-butylpyridine)erbium(III) (50%), and tris(3,5-di-*tert*-butylpyrazolato)(3,5-di-*tert*-butylpyrazole)erbium(III) (59%), respectively. Treatment of tris(cyclopentadienyl)lutetium(III) or tris(cyclopentadienyl)erbium(III) with 3,5-di-*tert*-butylpyrazole (3 equiv) and 4-*tert*-butylpyridine (2 equiv) in toluene at ambient temperature for 24 h afforded tris(3,5-di-*tert*-butylpyrazolato)bis(4-*tert*-butylpyridine)lutetium(III) (83%) and tris(3,5-di-*tert*-butylpyrazolato)bis(4-*tert*-butylpyridine)erbium(III) (41%), respectively. The X-ray crystal structures of all new complexes were determined. The X-ray structure analyses revealed seven- and eight-coordinate lanthanide complexes with all-nitrogen coordination spheres and η^2 -pyrazolato ligands. Molecular orbital calculations were carried out on dichloro(pyrazolato)diammineyttrium(III). The calculations demonstrate that η^2 -bonding of the pyrazolato ligand is favored over the η^1 -bonding mode and give insight into the bonding between yttrium and the pyrazolato ligands. Complexes bearing 3,5-di-*tert*-butylpyrazolato ligands can be obtained in a high state of purity and sublime without decomposition (150 °C, 0.1 mmHg). Application of these complexes as source compounds for chemical vapor deposition processes is discussed.

Introduction

There has been considerable interest in lanthanide-doped semiconductors, since the inclusion of small amounts of lanthanide ions ($\leq 1\%$) in semiconductor matrixes can provide sharp, temperature-independent luminescence from intrashell 4f transitions. Electrical stimulation of the host crystal would then lead to emission from the lanthanide centers. Such doped semiconductors have several important existing and anticipated technological applications. Erbium-doped semiconductors emit light at 1540 nm, resulting from the $^4I_{13/2} \rightarrow ^4I_{15/2}$ radiative transition of erbium(III). The energy of this emission corresponds to the minimum loss window of silicon optical fibers. As a result, erbium-doped semiconductor lasers have promising applications as fiber amplifiers and optical switches in optical fiber communication technology.²

Many different methods have been used to deposit lanthanide-doped semiconductor films.^{3–32} Liquid-phase epitaxy of erbium

- (1) (a) Wayne State University. (b) University of Delaware. (c) University of Wisconsin.
- (2) *Rare Earth Doped Semiconductors*; Pomreke, G. S., Klein, P. B., Langer, D. W., Eds.; Materials Research Society: Pittsburgh, PA, 1993; Volume 301.
- (3) *Rare Earth Doped Semiconductors II*; Coffa, S., Polman, A., Schwartz, R. N., Eds.; Materials Research Society: Pittsburgh, PA 1996; Vol. 422.

- (4) For a recent overview, see: Alcalá, R.; Cases, R. *Adv. Mater.* **1995**, *7*, 190.
- (5) Lai, M. Z.; Chang, L. B. *J. Appl. Phys.* **1992**, *72*, 1312.
- (6) Raczynska, J.; Fronc, K.; Langer, J. M.; Lemanska, A.; Stapor, A. *Appl. Phys. Lett.* **1988**, *53*, 761.
- (7) Bantien, F.; Bauser, B.; Weber, J. *J. Appl. Phys.* **1987**, *61*, 2803.
- (8) Torvik, J. T.; Qiu, C. H.; Feuerstein, R. J.; Pankove, J. I.; Namavar, F. *J. Appl. Phys.* **1997**, *81*, 6343.
- (9) Torvik, J. T.; Feuerstein, R. J.; Pankove, J. I.; Qiu, C. H.; Namavar, F. *Appl. Phys. Lett.* **1996**, *69*, 2098.
- (10) Silkowski, E.; Yeo, Y. K.; Hengehold, R. L.; Goldenberg, B.; Pomreke, G. S. *Mater. Res. Soc. Symp. Proc.* **1996**, *422*, 69.
- (11) Torvik, J. T.; Geuerstein, R. J.; Qiu, C. H.; Leksono, M. W.; Pankove, J. I.; Namavar, F. *Mater. Res. Soc. Symp. Proc.* **1996**, *422*, 199.
- (12) Qiu, C. H.; Leksono, M. W.; Pankove, J. I.; Torvik, J. T.; Feuerstein, R. J.; Namavar, F. *Appl. Phys. Lett.* **1995**, *66*, 562.
- (13) Wilson, R. G.; Schwartz, R. N.; Abernathy, C. R.; Pearton, S. J.; Newman, N.; Rubin, M.; Fu, T.; Zavada, J. M. *Appl. Phys. Lett.* **1994**, *65*, 992.
- (14) Polman, A. *J. Appl. Phys.* **1997**, *82*, 1.
- (15) Pomreke, G. S.; Ennen, H.; Haydl, W. *J. Appl. Phys.* **1986**, *59*, 601.
- (16) Nakata, J.; Jourdan, N.; Yamaguchi, H.; Takahei, K.; Yamamoto, Y.; Kido, Y. *J. Appl. Phys.* **1995**, *77*, 3095.
- (17) Seghier, D.; Benyattou, T.; Kalboussi, A.; Moneger, S.; Marrakchi, G.; Guillot, G.; Lambert, B.; Guivarc'h, A. *J. Appl. Phys.* **1994**, *75*, 4171.

into gallium arsenide (GaAs) cannot provide high doping levels of erbium, due to the low solubility of erbium in GaAs.^{5–7} Ion implantation can only provide high erbium concentrations in the region near the surface.^{8–15} Molecular beam epitaxy provides high lanthanide doping levels, but the lanthanide metals are highly reactive and difficult to keep pure.^{16–18} The method of choice for fabricating lanthanide-doped semiconductor films seems to be metal–organic vapor-phase epitaxy (MOVPE).^{19–25} The most widely used lanthanide sources are tris(cyclopentadienyl)lanthanide complexes and substituted derivatives thereof,^{19–25} although tris(acetylacetonato)- and tris(silyl)amide-based precursors have also been employed.^{26–32} Despite their success, existing lanthanide sources have low vapor pressures (typically ≤ 1 Torr at 200 °C). These low volatilities require high transport temperatures, which can lead to impurity incorporation and erratic doping levels. Moreover, known source compounds contain undesired elements bonded directly to erbium (carbon or oxygen) or in the coordination sphere (silicon), which can lead to the degradation of materials properties. The issue of adventitious elements is complicated, since defects bearing erbium–oxygen bonds may be important for efficient luminescence,^{22–25} but oxygen not complexed to erbium degrades the film properties. Finally, emission from erbium-doped semiconductor films is typically broad, suggesting that many different types of luminescent erbium sites are produced.^{14–32} The ideal precursor would introduce a single, highly emissive erbium site into the semiconductor matrix.

With these considerations in mind, we report the synthesis, structure, and properties of a series of lanthanide complexes bearing η^2 -pyrazolato ligands and neutral nitrogen donors. Deacon and co-workers have reported extensive studies of lanthanide complexes bearing η^2 -pyrazolato ligands and neutral oxygen donors.^{33–38} However, Deacon's compounds may be

unsuitable for use in group 13 compound semiconductor matrixes due to the oxygen content and because the complexes apparently decompose with loss of the neutral oxygen donor ligands upon attempted sublimation.^{33,34} By contrast, the lanthanide complexes described herein sublime without decomposition and are thermally stable to nearly 300 °C. Furthermore, molecular orbital calculations have been carried out on model yttrium complexes, and provide detailed insight into the bonding between lanthanide metal centers and pyrazolate donors. We have recently reported that use of one of the complexes described below, tris(3,5-di-*tert*-butylpyrazolato)bis(4-*tert*-butylpyridine)erbium(III), as the erbium source in an MOVPE process results in highly emissive erbium-doped gallium arsenide films.^{39–41} Importantly, this precursor affords films with sharp luminescence from a single type of erbium emitting center, while cyclopentadienyl-based source compounds give broad emission from many types of emitting sites. Therefore, the compounds described herein represent a very promising new class of lanthanide precursors for use in chemical vapor deposition (CVD) processes.

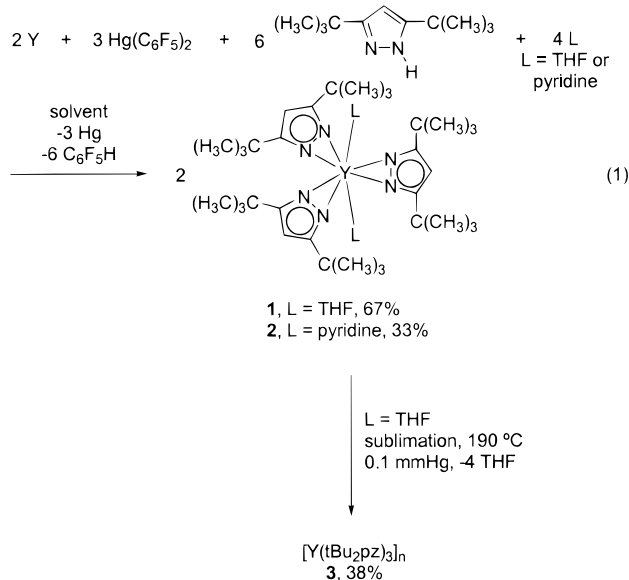
Results

Search for Thermally Stable, Volatile, and Monomeric Structures. Our first goal was to identify ligands for lanthanide complexes that would afford volatile, thermally stable compounds that could be used as sources in CVD processes. Additionally, we sought complexes with all-nitrogen coordination spheres that contained only the lanthanide ion, nitrogen, carbon, and hydrogen to minimize the incorporation of undesired elements into the semiconductor matrix. Deacon and co-workers reported that monomeric tris(η^2 -3,5-di-*tert*-butylpyrazolato)bis(tetrahydrofuran)neodymium(III) volatilized, but appeared to lose the tetrahydrofuran ligands in the process.^{33,34} We reasoned that the use of neutral donor ligands that are more basic than tetrahydrofuran might yield complexes with improved thermal stability. To probe this point in more detail, tris(η^2 -3,5-di-*tert*-butylpyrazolato)bis(tetrahydrofuran)yttrium(III) (**1**) was prepared using the method of Deacon with tetrahydrofuran as the solvent (eq 1).³⁴ The analogous complex tris(η^2 -3,5-di-*tert*-butylpyrazolato)bis(pyridine)yttrium(III) (**2**; 33%) was synthesized by a similar procedure, except that the reaction was conducted in toluene and pyridine was added to cap the coordination sphere. The new complex **2** was characterized by spectral and analytical methods. In addition, the monomeric nature of **2** in the solid state was established by X-ray crystallography (vide infra).

To evaluate the thermal stability of **1** and **2**, sublimations were carried out. The attempted sublimation (180–190 °C, 0.1 mmHg) of **1** for 18 h afforded tris(3,5-di-*tert*-butylpyrazolato)yttrium(III) (**3**; 38%, eq 1) as a white solid. Characterization of **3** by spectroscopic and analytical techniques clearly indicated the loss of tetrahydrofuran during the sublimation process. Alternatively, **1** lost coordinated tetrahydrofuran in the solid state and then sublimed as **3**. The yield of **3** from **1** was only 38%, indicating extensive decomposition of **1** during vapor transport. The X-ray crystal structure of **3** could not be determined because crystals of sufficient quality could not be grown. However, **3** was markedly less soluble than **1**, suggesting dimeric or polymeric structures with bridging pyrazolato ligands.

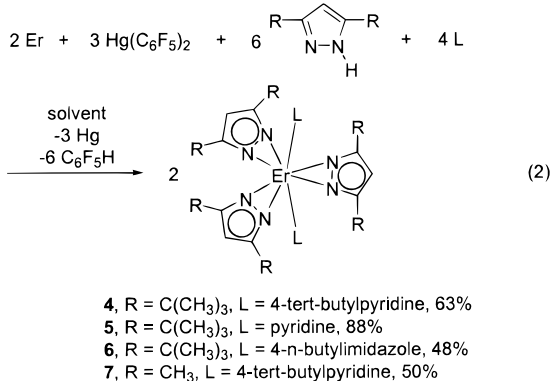
- (18) Ennen, H.; Wagner, J.; Muller, H. D.; Smith, R. S. *J. Appl. Phys.* **1987**, *61*, 4877.
 (19) Nukeaw, J.; Tanagisawa, J.; Matsubara, N.; Fujiwara, Y.; Takeda, Y. *Appl. Phys. Lett.* **1997**, *70*, 84.
 (20) Redwing, J. M.; Kuech, T. F.; Gordon, D. C.; Vaarstra, B. A.; Lau, S. S. *J. Appl. Phys.* **1994**, *76*, 1585.
 (21) Pearton, S. J.; Abernathy, C. R.; MacKenzie, J. D.; Schwartz, J. D.; Wilson, R. G.; Zavada, J. M.; Shul, R. J. *Mater. Res. Soc. Symp. Proc.* **1996**, *422*, 47.
 (22) Hogg, R. A.; Takahei, K.; Taguchi, A. *J. Appl. Phys.* **1996**, *79*, 8682.
 (23) Taguchi, A.; Takahei, K. *J. Appl. Phys.* **1996**, *79*, 4330.
 (24) Chang, S. J.; Takahei, K. *Appl. Phys. Lett.* **1994**, *65*, 433.
 (25) Taniguchi, M.; Takahei, K. *J. Appl. Phys.* **1993**, *73*, 943.
 (26) Wang, X. Z.; Wessels, B. W. *Appl. Phys. Lett.* **1994**, *64*, 1537.
 (27) Williams, D. M.; Wessels, B. W. *Appl. Phys. Lett.* **1990**, *56*, 566.
 (28) Morse, M.; Zheng, B.; Palm, J.; Duan, X.; Kimerling, L. C. *Mater. Res. Soc. Symp. Proc.* **1996**, *422*, 41.
 (29) Andry, P. S.; Varhue, W. J.; Adams, E.; Lavoie, M.; Klein, P. B.; Hengehold, R.; Hunter, J. *Mater. Res. Soc. Symp. Proc.* **1996**, *422*, 57.
 (30) Andry, P. S.; Varhue, W. J.; Lapido, F.; Ahmed, K.; Adams, E.; Lavoie, M.; Klein, P. B.; Hengehold, R.; Hunter, J. *J. Appl. Phys.* **1996**, *80*, 551.
 (31) Rees, W. S., Jr.; Lay, U. W.; Greenwald, A. C. *Mater. Res. Soc. Symp. Proc.* **1993**, *301*, 21.
 (32) Greenwald, A. C.; Linden, K. J.; Rees, W. S., Jr.; Just, O.; Haegel, N. M.; Donder, S. *Mater. Res. Soc. Symp. Proc.* **1996**, *422*, 63.
 (33) Cosgriff, J. E.; Deacon, G. B.; Gatehouse, B. M.; Hemling, H.; Schumann, H. *Angew. Chem., Int. Ed. Engl.* **1993**, *32*, 874.
 (34) Cosgriff, J. E.; Deacon, G. B.; Gatehouse, B. M.; Hemling, H.; Schumann, H. *Aust. J. Chem.* **1994**, *47*, 1223.
 (35) Cosgriff, J. E.; Deacon, G. B.; Gatehouse, B. M. *Aust. J. Chem.* **1993**, *46*, 1881.
 (36) Cosgriff, J. E.; Deacon, G. B.; Fallon, G. D.; Gatehouse, B. M.; Schumann, H.; Weimann, R. *Chem. Ber.* **1996**, *129*, 953.
 (37) Deacon, G. B.; Delbridge, E. E.; Skelton, B. W.; White, A. H. *Eur. J. Inorg. Chem.* **1998**, 543.
 (38) Cosgriff, J. E.; Deacon, G. B.; Gatehouse, B. M.; Lee, P. R.; Schumann, H. *Z. Anorg. Allg. Chem.* **1996**, *622*, 1399.

- (39) Culp, T. D.; Cederberg, J. G.; Bieg, B.; Kuech, T. F.; Bray, K. L.; Pfeiffer, D.; Winter, C. H. *J. Appl. Phys.* **1998**, *83*, 4918.
 (40) Cederberg, J. G.; Culp, T. D.; Bieg, B.; Pfeiffer, D.; Winter, C. H.; Bray, K. L.; Kuech, T. F. *J. Cryst. Growth* **1998**, *195*, 105.
 (41) Cederberg, J. G.; Culp, T. D.; Bieg, B.; Pfeiffer, D.; Winter, C. H.; Bray, K. L.; Kuech, T. F. *J. Appl. Phys.* **1999**, *85*, 1825.



By contrast, **2** sublimed at 150 °C (0.1 mmHg) without a visible residue. The ^1H and $^{13}\text{C}\{^1\text{H}\}$ NMR spectra of sublimed **2** were identical to those of material that was purified by crystallization. The stability of **2** suggested that replacement of the neutral oxygen donors in **1** with pyridine ligands leads to a dramatic increase in thermal stability.

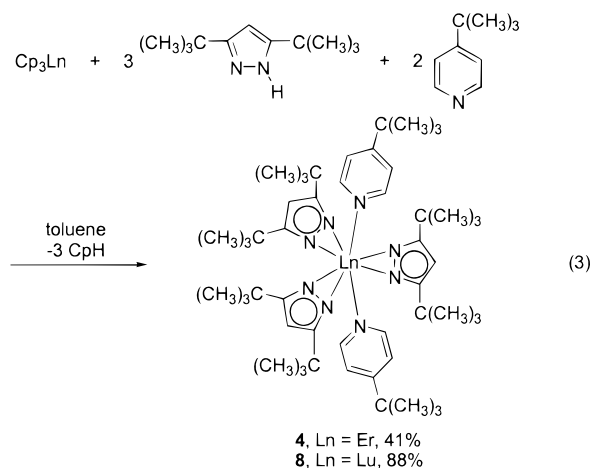
Synthesis of Pyrazolato Complexes of Yttrium, Lutetium, and Erbium. In view of the remarkable thermal stability of **2** and its low-temperature sublimation, a series of bright pink erbium pyrazolato complexes **4–7** was prepared using a synthetic method similar to that used for **2** (eq 2). The structural



assignments of **4–7** were based upon spectral and analytical data. In addition, X-ray crystal structures of these complexes confirmed monomeric formulations (vide infra). Interestingly, **4** and **7** are monomeric with three η^2 -pyrazolato ligands, while the analogous tetrahydrofuran adducts of neodymium(III) are monomeric with di-*tert*-butylpyrazolato ligands but dimeric with two μ_2 -pyrazolato ligands per dimer unit when dimethylpyrazolato ligands are present.⁵⁰ The better donor characteristics of

the 4-*tert*-butylpyridine ligands, compared to tetrahydrofuran ligands, must promote the formation of a monomeric structure in the case of **7**. Like **2**, the 3,5-di-*tert*-butylpyrazolato complexes **4–6** sublime without decomposition at 150 °C (0.1 mmHg). However, the 3,5-dimethylpyrazolato complex **7** decomposed under the same conditions without sublimation. Hence, the bulky *tert*-butyl substituents on the pyrazolato ligands appear to be required to achieve thermal stability and volatility, whereas the presence of alkyl groups on the neutral nitrogen donor ligands does not have a noticeable effect on the sublimation abilities of **4–6**. The sublimation of **4** was studied carefully. In a preparative scale sublimation study of analytically pure **4** (0.5 g), very little residue ($\leq 0.8\%$) was observed at the finish of the sublimation and 88% of **4** was isolated as sublimed material.

The preparation of pyrazolato complexes from tris(cyclopentadienyl)lanthanide(III) complexes was briefly investigated (eq 3). Motivations for investigating this alternative synthetic



procedure included a desire to avoid working with large amounts of bis(pentafluorophenyl)mercury, the fact that tris(cyclopentadienyl)lanthanide(III) complexes can be obtained in high purity by several sublimations, and the desire to use the minimum number of reagents in future preparations of high-purity source compounds. In an initial experiment, tris(cyclopentadienyl)erbium(III) was reacted with 3,5-di-*tert*-butylpyrazole (3 equiv) and 4-*tert*-butylpyridine (2 equiv) in toluene. After 24 h at ambient temperature, **4** was isolated in 41% yield as pink crystals. Analogous treatment of tris(cyclopentadienyl)lutetium(III) afforded **8** in 83% yield as a colorless solid. Examination of the crude product by ^1H NMR spectroscopy revealed complete consumption of cyclopentadienyl lutetium species, indicating that the reaction was complete at this time. The identity of **4** was confirmed by comparison of its melting point and infrared spectrum with those obtained for material prepared according to eq 2. The structure of **8** was established by spectral and analytical techniques, and by X-ray crystallography. We did not pursue further syntheses using cyclopentadienyl starting materials. However, the preparations of **4** and **8** demonstrate the utility of this methodology. Interestingly, a previous study reported that only two cyclopentadienyl ligands were replaced upon treatment of tris(cyclopentadienyl)lanthanide(III) complexes with pyrazoles.^{42,43}

(42) Zhou, X.; Ma, W.; Huang, Z.; Cai, R.; You, X.; Huang, X. *J. Organomet. Chem.* **1997**, *545*, 309.

(43) Zhou, X.; Ma, H.; Huang, X.; You, X. *J. Chem. Soc., Chem. Commun.* **1995**, 2483.

(44) Cosgriff, J. E.; Deacon, G. B. *Angew. Chem., Int. Ed.* **1998**, *37*, 286.

(45) Pfeiffer, D.; Heeg, M. J.; Winter, C. H. *Angew. Chem., Int. Ed.* **1998**, *37*, 2517.

(46) Guzei, I. A.; Baboul, A. G.; Yap, G. P. A.; Rheingold, A. L.; Schlegel, H. B.; Winter, C. H. *J. Am. Chem. Soc.* **1997**, *119*, 3387.

(47) Guzei, I. A.; Yap, G. P. A.; Winter, C. H. *Inorg. Chem.* **1997**, *36*, 1738.

(48) Guzei, I. A.; Winter, C. H. *Inorg. Chem.* **1997**, *36*, 4415.

(49) Yélamos, C.; Heeg, M. J.; Winter, C. H. *Inorg. Chem.* **1999**, *38*, 1871.

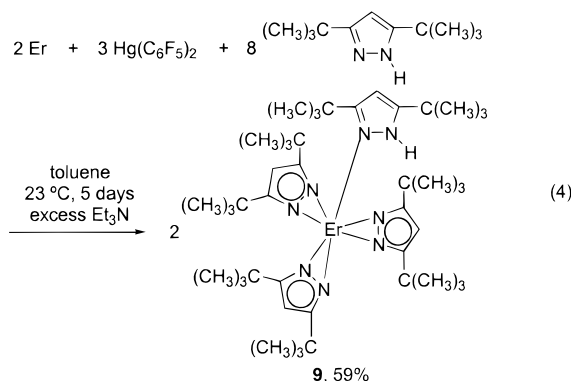
(50) Deacon, G. B.; Gatehouse, B. M.; Nickel, S.; Platts, S. N. *Aust. J. Chem.* **1991**, *44*, 613.

Table 1. Crystal Data and Data Collection Parameters for **2**, **4**, **7**, **8**, and **9**

	2	4	7	8	9
empirical formula	C ₄₃ H ₆₇ N ₈ Y	C ₅₁ H ₈₃ N ₈ Er	C ₃₃ H ₄₇ N ₈ Er	C ₅₁ H ₈₃ LuN ₈	C ₄₄ H ₇₇ N ₈ Er
fw	784.96	975.51	723.05	983.22	885.40
space group	<i>P2₁/c</i>	<i>Pbca</i>	<i>P4₁2₁</i>	<i>Pbca</i>	<i>P2₁/c</i>
<i>a</i> (Å)	11.9987(6)	19.0270(6)	13.6404(3)	19.0520(10)	20.9714(3)
<i>b</i> (Å)	19.7512(9)	21.5576(8)	21.6580(10)	10.6371(2)	
<i>c</i> (Å)	20.2069(9)	26.6172(9)	19.1118(4)	26.6770(10)	22.1332(1)
β (deg)	101.7470(10)	93.397(1)			
<i>V</i> (Å ³)	4688.5(4)	10917.7(6)	3555.95(13)	11007.7(9)	4928.69(12)
<i>Z</i>	4	8	4	8	4
<i>T</i> (°C)	22(5)	-54(2)	-55(2)	22(2)	-55(2)
λ (Å)	0.710 73	0.710 73	0.710 73	0.710 73	0.710 73
ρ (calcd) (g cm ⁻³)	1.112	1.187	1.351	1.187	1.193
μ (mm ⁻¹)	1.279	1.575	2.392	1.831	1.738
<i>R</i> (<i>F</i>) (%)	6.62 ^a	3.09 ^b	2.69 ^b	4.89 ^a	2.98 ^b
<i>Rw</i> (<i>F</i>) (%)	12.82 ^a	8.81 ^b	5.01 ^b	9.79 ^a	8.08 ^b

$$^a R(F) = \frac{\sum ||F_o| - |F_c||}{\sum |F_o|}; R_w(F) = \frac{[\sum w(F_o^2 - F_c^2)^2 / \sum w(F_o^2)^2]^{1/2}}{\sum w(F_o^2)^2}^{1/2}; ^b R(F) = \frac{(\sum |\Delta F|)}{\sum |F_o|}; R_w(F) = \frac{[\sum w|\Delta F|^2 / \sum w(F_o^2)^2]^{1/2}}{\sum w(F_o^2)^2}^{1/2}$$

We next sought to determine if tertiary alkylamines could be used as the neutral donor ligands in lanthanide pyrazolato complexes. Accordingly, erbium metal was treated with bis-(pentafluorophenyl)mercury, 3,5-di-*tert*-butylpyrazole, and excess triethylamine in toluene at ambient temperature for 5 days according to eq 4. Workup afforded tris(3,5-di-*tert*-butylpyra-



zolato)(3,5-di-*tert*-butylpyrazolato)erbium(III) (**9**; 59%) as a bright pink crystalline solid. Complex **9** was characterized by spectral and analytical methods, and its structure was determined by X-ray crystallography. Surprisingly, there were no triethylamine ligands in **9**. Instead, the complex was found to contain three η^2 -pyrazolato ligands and one η^1 -bonded 3,5-di-*tert*-butylpyrazole ligand. Several experiments were conducted to probe the formation of **9**. If the reaction was conducted without triethylamine, no tractable lanthanide complexes could be isolated after 120 h. This experiment indicates that triethylamine plays a crucial role in the reaction. If the reaction was conducted with a 3:1 molar ratio of 3,5-di-*tert*-butylpyrazole to erbium metal in the presence of triethylamine, then **9** was the only product isolated, but the yield was reduced from that observed with the 4:1 stoichiometry. We propose that triethylamine coordinates very weakly to the bulky tris(3,5-di-*tert*-butylpyrazolato)erbium(III) fragment due to steric interactions between the amine ethyl groups and the pyrazolato *tert*-butyl groups; i.e., the cone angle of triethylamine is too large to allow strong bonding to the axial coordination sites. Due to the weak coordination of triethylamine, 3,5-di-*tert*-butylpyrazole becomes the best donor ligand available and reacts with the tris(3,5-di-*tert*-butylpyrazolato)erbium(III) fragment to form **9**. Complexes similar to **9** have not been described, although the complex La(tBu₂pZ)₃(tBu₂pZH)₂ has been claimed in a review paper.⁴⁴

Crystal Structures of 2, 4, 7, 8, and 9. The X-ray crystal structures of **2**, **4**, **7**, **8**, and **9** were determined to establish their

Table 2. Selected Bond Lengths (Å) and Angles (deg) for **2**

Y-N(1)	2.532(3)	Y-N(5)	2.405(3)
Y-N(2)	2.390(3)	Y-N(6)	2.341(3)
Y-N(3)	2.336(3)	Y-N(7)	2.323(3)
Y-N(4)	2.323(3)	Y-N(8)	2.503(3)
N(1)-Y-N(8)	146.31(10)	N(1)-Y-N(6)	92.22(10)
N(7)-Y-N(8)	86.75(10)	N(2)-Y-N(5)	109.68(10)

Table 3. Selected Bond Lengths (Å) and Angles (deg) for **4**

Er-N(1)	2.485(4)	Er-N(5)	2.333(4)
Er-N(2)	2.484(4)	Er-N(6)	2.367(4)
Er-N(3)	2.320(4)	Er-N(7)	2.396(4)
Er-N(4)	2.330(4)	Er-N(8)	2.315(4)
N(1)-Er-N(2)	153.03(14)	N(1)-Er-N(3)	85.8(14)
N(2)-Er-N(4)	86.1(14)	N(6)-Er-N(7)	106.1(14)

Table 4. Selected Bond Lengths (Å) and Angles (deg) for **7**

Er-N(1)	2.367(4)	Er-N(1A)	2.367(4)
Er-N(2)	2.319(4)	Er-N(2A)	2.319(4)
Er-N(3)	2.335(4)	Er-N(3A)	2.335(4)
Er-N(4)	2.476(4)	Er-N(4A)	2.476(4)
N(4)-Er-N(4A)	162.6(14)	N(3)-Er-N(4)	86.4(14)
N(3A)-Er-N(4A)	86.4(14)	N(2)-Er-N(2A)	91.3(14)

Table 5. Selected Bond Lengths (Å) and Angles (deg) for **8**

Lu-N(1)	2.455(4)	Lu-N(5)	2.299(4)
Lu-N(2)	2.462(4)	Lu-N(6)	2.300(4)
Lu-N(3)	2.371(4)	Lu-N(7)	2.294(4)
Lu-N(4)	2.294(4)	Lu-N(8)	2.342(4)
N(1)-Lu-N(2)	153.01(14)	N(1)-Lu-N(5)	85.96(14)
N(2)-Lu-N(6)	86.15(14)	N(3)-Lu-N(8)	105.27(14)

Table 6. Selected Bond Lengths (Å) and Angles (deg) for **9**

Er-N(1)	2.405(4)		
Er-N(2)	2.204(4)	Er-N(6)	2.560(4)
Er-N(3)	2.457(4)	Er-N(7)	2.194(4)
Er-N(4)	2.304(4)	Er-N(8)	2.212(4)
N(1)-Er-N(6)	81.0(14)	N(2)-Er-N(6)	101.6(14)
N(3)-Er-N(6)	93.4(14)	N(4)-Er-N(6)	126.8(14)
N(7)-Er-N(6)	110.8(14)	N(8)-Er-N(6)	87.4(14)

molecular geometries. Experimental crystallographic data are summarized in Table 1. Selected bond lengths and angles are given in Tables 2–6, while perspective views are presented in Figures 1–5. Further data are available in the Supporting Information. The crystal structures of **5** and **6** were also determined; these data are deposited in the Supporting Information.

Compound **2** exists as an eight-coordinate, monomeric complex with three pyrazolato ligands bound by their nitrogen atoms in η^2 -fashion (Figure 1). The coordination geometry about yttrium can be envisioned as distorted trigonal bipyramidal, if

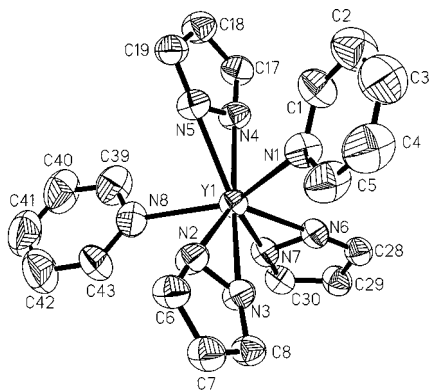


Figure 1. Perspective view of tris(3,5-di-*tert*-butylpyrazolato)bis(pyridine)yttrium(III) (**2**) with thermal ellipsoids at the 50% probability level. The *tert*-butyl groups have been removed for clarity.

the centers of the nitrogen–nitrogen bonds of the η^2 -pyrazolato ligands are considered to be monodentate donors. The pyridine ligands are located in the axial positions, whereas the three pyrazolato donors occupy the equatorial plane. Two pyrazolato ligands and the yttrium metal define the equatorial plane, while the third pyrazolato ligand is approximately perpendicular to this plane. The distorted trigonal bipyramidal geometry is characterized by N(1)–Y–N(8), N(1)–Y–N(6), N(7)–Y–N(8), and N(2)–Y–N(5) angles of 146.31(10), 92.22(10), 86.75(10), and 109.68(10)°, respectively. This distortion is probably caused by steric interactions between the *tert*-butyl groups of the 3,5-di-*tert*-butylpyrazolato ligands. The yttrium–nitrogen bond lengths fall between 2.323(3) and 2.405(3) Å for the pyrazolato ligands and between 2.503(3) and 2.532(3) Å for the pyridine donor. These values compare well with other η^2 -pyrazolato lanthanide–nitrogen bond lengths found in Ln-(tBu₂pz)₃(THF)₂ (Ln = Nd, 2.381(8)–2.492(9) Å; Ln = Er, 2.274(7)–2.386(8) Å).^{33,34} The η^2 -pyrazolato ligands in **2** are asymmetrically bonded with a difference in yttrium–nitrogen bond lengths of 0.082 Å. We have previously documented similar “slipped” η^2 -pyrazolato coordination in magnesium, titanium, and tantalum complexes.^{45–49} The slipped η^2 -bonding probably originates from steric interactions involving the *tert*-butyl groups. Complex **2** possesses a structure that is similar to tris(η^2 -pyrazolato)bis(tetrahydrofuran)lanthanide complexes that have been described by Deacon;^{33,34} however, **2** is the first structurally characterized complex of yttrium bearing η^2 -pyrazolato ligands.

Compound **4** is monomeric with three η^2 -pyrazolato ligands and two 4-*tert*-butylpyridine ligands (Figure 2). The distorted trigonal bipyramidal coordination geometry, assuming that the centers of the nitrogen–nitrogen bonds of the η^2 -pyrazolato ligands are treated as monodentate donors, is characterized by N(1)–Er–N(2), N(1)–Er–N(3), N(2)–Er–N(4), and N(6)–Er–N(7) angles of 153.03(14), 85.8(14), 86.1(14), and 106.1(14)°, respectively. The distortion is probably due to steric interactions involving the *tert*-butyl groups of the 3,5-di-*tert*-butylpyrazolato ligands. The erbium–nitrogen bond lengths range between 2.315(4) and 2.396(4) Å for the pyrazolato ligands and are 2.484(4) and 2.485(4) Å for the 4-*tert*-butylpyridine donors.

Compound **7** possesses a molecular structure similar to those of **2** and **4**. It is a monomeric, eight-coordinate compound with three η^2 -pyrazolato ligands and two 4-*tert*-butylpyridine ligands (Figure 3). The molecule of **7** occupies a crystallographic 2-fold axis. Distortion from approximate trigonal bipyramidal geometry is demonstrated by N(4)–Er–N(4A), N(3)–Er–N(4), N(3A)–

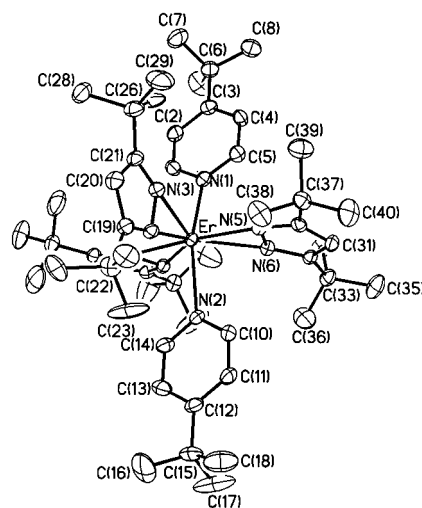


Figure 2. Perspective view of tris(3,5-di-*tert*-butylpyrazolato)bis(4-*tert*-butylpyridine)erbium(III) (**4**) with thermal ellipsoids at the 30% probability level.

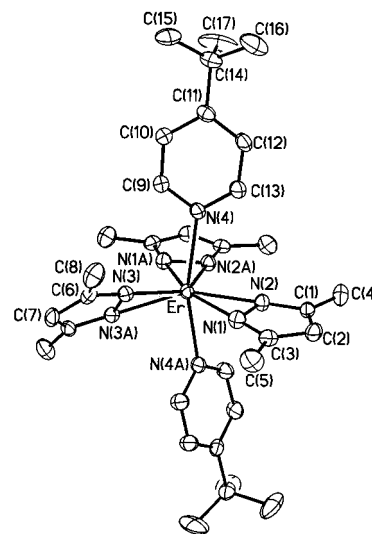


Figure 3. Perspective view of tris(3,5-dimethylpyrazolato)bis(4-*tert*-butylpyridine)erbium(III) (**7**) with thermal ellipsoids at the 30% probability level.

Er–N(4A), and N(2)–Er–N(2A) angles of 162.6(14), 86.4(14), 86.4(14), and 91.3(14)°, respectively. These values are closer to idealized trigonal bipyramidal geometry than the related values in **2** and **4**, due to the smaller steric profile of the methyl substituents on the pyrazolato ligands. The erbium–nitrogen bond lengths range between 2.319(4) and 2.367(4) Å for the pyrazolato ligands, and that for the 4-*tert*-butylpyridine donors is 2.476(4) Å. The decreased asymmetry of the erbium–nitrogen bond lengths associated with the η^2 -pyrazolato donors also demonstrates that the coordination sphere is sterically less saturated than in **2** and **4**. The monomeric structure of complex **7** is unusual, since lanthanide derivatives bearing 3,5-dimethylpyrazolato ligands are dimeric, or more aggregated, with both terminal η^2 -bonding and μ - η^2 -bridging bonding modes.^{50–53}

Complex **8** crystallized as a monomeric complex with distorted trigonal bipyramidal geometry, if the centers of the

(51) Schumann, H.; Lee, P. R.; Löbel, J. *Angew. Chem., Int. Ed. Engl.* **1989**, *28*, 1033.

(52) Schumann, H.; Löbel, J.; Pickardt, J.; Qian, C.; Xie, Z. *Organometallics* **1991**, *10*, 215.

(53) Anwander, R. *Top. Curr. Chem.* **1996**, *179*, 76.

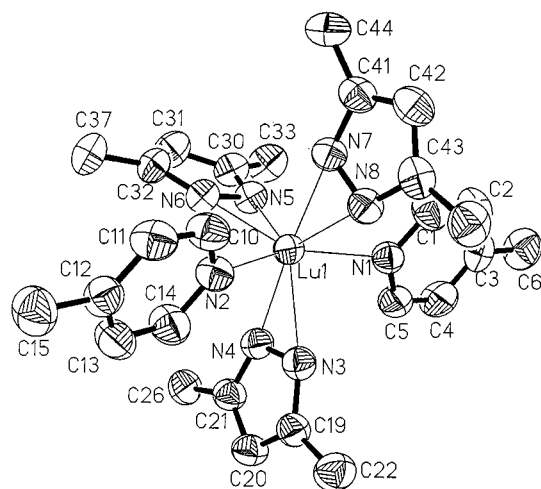


Figure 4. Perspective view of tris(3,5-di-*tert*-butylpyrazolato)bis(4-*tert*-butylpyridine)lutetium(III) (**8**) with thermal ellipsoids at the 50% probability level. The *tert*-butyl methyl groups have been removed for clarity.

nitrogen–nitrogen bonds in the η^2 -pyrazolato ligands are considered to be monodentate donors. The coordination sphere contains three η^2 -pyrazolato ligands and two 4-*tert*-butylpyridine ligands (Figure 4). The distorted coordination geometry was characterized by N(1)–Lu–N(2), N(1)–Lu–N(5), N(2)–Lu–N(6), and N(3)–Lu–N(8) angles of 153.01(14), 85.96(14), 86.15(14), and 105.27(14)°, respectively. The lutetium–nitrogen bond lengths fall between 2.294(4) and 2.371(4) Å for the pyrazolato ligands and are 2.455(4) and 2.462(4) Å for the 4-*tert*-butylpyridine donors. The asymmetry of bond lengths associated with the pyrazolato ligands in **8** (range 0.077 Å) is similar to the value found in **2**. The almost identical geometries of **2** and **8** are probably due to the similar size of the yttrium(III) ion (radius 0.900 Å) and lutetium(III) ion (ionic radius 0.861 Å).⁵⁴ Complex **8** is the first structurally characterized complex of lutetium containing η^2 -pyrazolato ligands.

Compound **9** exists as a seven-coordinate, monomeric complex with three pyrazolato ligands bound by their nitrogen atoms in η^2 -fashion and one 3,5-di-*tert*-butylpyrazole donor bonded to the erbium center in an η^1 -fashion (Figure 5). The coordination geometry about erbium can be envisioned as distorted tetrahedral, if the centers of the nitrogen–nitrogen bonds in the η^2 -pyrazolato ligands are considered to be monodentate donors. The distorted tetrahedral geometry is characterized by N(1)–Er–N(6), N(2)–Er–N(6), N(3)–Er–N(6), N(4)–Er–N(6), N(6)–Er–N(7), and N(6)–Er–N(8) angles of 81.0(14), 101.6(14), 93.4(14), 126.8(14), 110.8(14), and 87.4(14)°, respectively. The erbium–nitrogen bond lengths range between 2.204(4) and 2.457(4) Å for the pyrazolato ligands, and that for the 3,5-di-*tert*-butylpyrazole donor is 2.560(4) Å. The large asymmetry of the erbium–nitrogen bond lengths associated with the η^2 -pyrazolato ligands (range 0.253 Å) illustrates the extreme steric crowding that is present in the coordination sphere of **9**. Unfavorable steric interactions are undoubtedly the reason that there is only one neutral donor ligand in **9**.

Purification Procedure and Analysis of 4 by Inductively Coupled Plasma Optical Emission Spectroscopy. The samples of **4** that were studied came from large-scale syntheses that had been conducted to provide sufficient material for CVD studies.

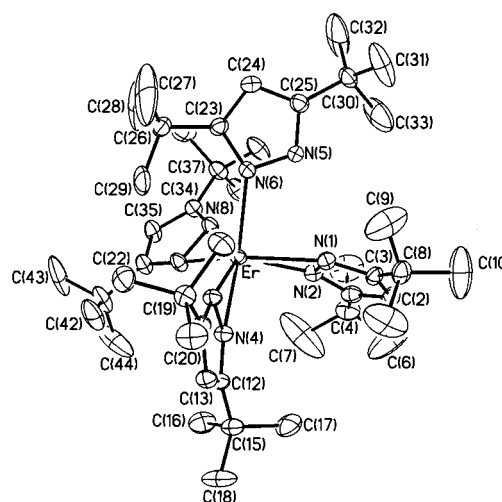


Figure 5. Perspective view of tris(3,5-di-*tert*-butylpyrazolato)(3,5-di-*tert*-butylpyrazole)erbium(III) (**9**) with thermal ellipsoids at the 30% probability level.

Samples of **4** had been sublimed two times, while the erbium metal was used as received from a commercial source. Inductively coupled plasma optical emission spectroscopy (ICP-OES) was used to determine the purity of **4** and the erbium metal used to prepare **4**, with regard to 50 elements that were potential contaminants. A complete list of the elements that were screened is given in the Supporting Information, and includes all of the lanthanide metals and many transition metal and main group elements. The results are derived from two different lots of 99.9% erbium metal and several different preparations of **4** using erbium metal from these two lots. For each element, five potential spectroscopic lines were examined for detection limits, sensitivity, linearity, range, and possible interferences. The best line was selected on the basis of optimization of these factors. The results represent the average of four different samples each of erbium metal and **4**. Various approaches to background correction were employed, again to optimize results. The reported results are in parts per million (derived from % w/w determination). The major contaminants in the erbium metal were the lanthanide elements thulium (727 ppm), yttrium (502 ppm), lutetium (261 ppm), europium (215 ppm), and holmium (146 ppm), with traces of neodymium (9.66 ppm), samarium (7.23 ppm), and lanthanum (1.29 ppm). Main group and transition metals that were present included sodium (144 ppm), silver (965 ppm), magnesium (48.9 ppm), copper (29.9 ppm), and potassium (17.9 ppm). In addition, a significant concentration of thorium (162 ppm) was detected. The results demonstrate that **4** is significantly purer than the erbium metal used in its synthesis. The major contaminants in **4** include the lanthanide metals yttrium (76.8 ppm), europium (47.9 ppm), lutetium (41.8 ppm), and holmium (1.89 ppm), although the levels of these elements were significantly reduced from those observed in the erbium metal. Given the similar sizes of erbium and these lanthanide elements,⁵⁴ it is likely that complexes of the formula Ln(*t*Bu₂pz)₃(4-*tert*-butylpyridine)₂ (Ln = Y, Eu, Lu, Ho) are formed during the preparation of **4** and are transported along with **4** during the sublimations. Other elements that were observed in **4** include small amounts of mercury (9.78 ppm), phosphorus (6.12 ppm), potassium (5.27 ppm), and thorium (5.09 ppm). The mercury was absent in the erbium metal samples, and likely is a residue of the synthetic method leading to **4**. The concentrations of thorium and potassium were significantly reduced from the erbium metal.

(54) Greenwood, N. N.; Earnshaw, A. *Chemistry of the Elements*, 2nd ed.; Butterworth-Heinemann: Oxford, 1997; pp 946, 1233.

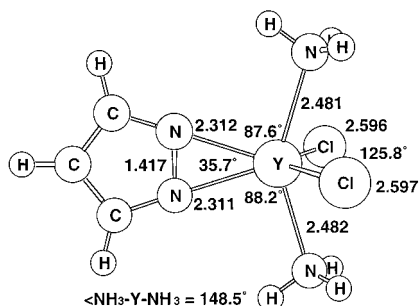


Figure 6. Optimized geometry of dichloro(η^2 -pyrazolato)diammineyttrium(III) (**10**) calculated at the B3LYP/LANL2DZ level of theory.

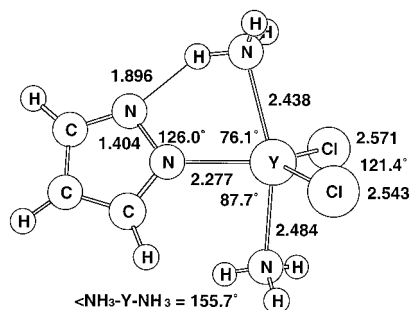


Figure 7. Optimized geometry of dichloro(η^1 -pyrazolato)diammineyttrium(III) (**11**) calculated at the B3LYP/LANL2DZ level of theory with the yttrium–nitrogen–nitrogen angle fixed at 126°.

Molecular Orbital Calculations on Yttrium(III) Complexes Bearing a Pyrazolato Ligand. To understand the bonding between the lanthanide ions and the pyrazolato ligands, we conducted molecular orbital calculations on the model complexes dichloro(η^2 -pyrazolato)diammineyttrium (**10**) and dichloro(η^1 -pyrazolato)diammineyttrium (**11**) at the B3LYP/

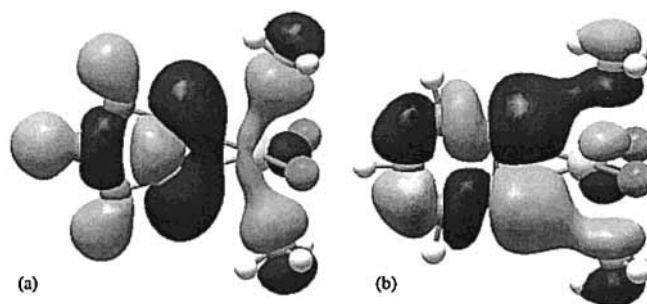
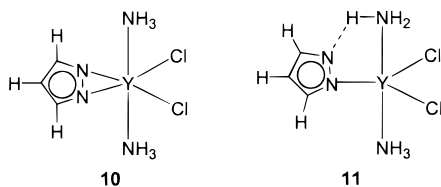


Figure 8. Molecular orbitals of dichloro(η^2 -pyrazolato)diammineyttrium(III) (**10**) containing the (a) symmetric and (b) antisymmetric combinations of the pyrazolato nitrogen lone pairs of electrons.

bond between the uncoordinated nitrogen of the pyrazolato ligand and the adjacent ammonia. The strength of such hydrogen bonds is typically 5–10 kcal/mol. This suggests that η^2 -pyrazolato bonding may be favored by up to 20 kcal/mol over the η^1 -pyrazolato coordination mode in the absence of hydrogen bonding.

Natural population analysis showed that the bonding in **10** is considerably more ionic than that in the titanium–pyrazolato complex trichloro(3,5-dimethylpyrazolato)titanium(IV), for which we have recently reported molecular orbital calculations.⁴⁶ The charge on the pyrazolato ligand in **10** is -0.75 , compared to -0.32 in the titanium case. The chlorine atoms in **10** are also more negative (-0.63 versus -0.32 to -0.35) than in the titanium complex. The charge distribution in **11** is similar to that in **10**. Examination of the molecular orbitals of **10** reveals features similar to those of the titanium–pyrazolato complex. As shown in Figure 8, the pyrazolato ligand interacts via symmetric and antisymmetric combinations of the in-plane nitrogen lone pairs. In contrast to the titanium case, these orbitals in **10** show relatively little participation from the yttrium d orbitals. This is consistent with more ionic bonding in the yttrium–pyrazolato complexes than in titanium–pyrazolato complexes.

Discussion

A significant discovery in the present study is the remarkable thermal stability of the pyrazolato complexes **2–9**, compared to the much lower thermal stability of **1** and related compounds reported by Deacon that contain tetrahydrofuran as the neutral donor ligand. The pyridine- and imidazole-based donor ligands in **2–9** are substantially stronger Lewis bases than tetrahydrofuran, and the increased bond strength associated with the nitrogen donors is probably the dominant contribution to the increase in thermal stability of **2–9**, compared to **1**. As an illustration of the properties of the new complexes, **4** melts sharply at 241 °C to afford a pink liquid that is stable for at least 0.25 h in a sealed capillary under argon at 300 °C. Sublimation of **4** occurs at 150 °C (0.1 mmHg) to afford an 88% recovery of **4** with <0.8% residue in the sublimation vessel. By contrast, Cp₃Er sublimes at 180–190 °C (0.1 mmHg) in the same apparatus used to sublime **4**. Therefore, **4** appears to be more volatile than Cp₃Er.

The results of the molecular orbital calculations on the model complex **10** indicate that the bonding between the pyrazolato ligands and the lanthanide ions is substantially ionic. Therefore, the key to obtaining a low lattice energy, and hence the highest possible volatility, is to encapsulate the lanthanide ion with bulky ligands that reduce intermolecular attractive forces. In **2–9**, it was found that complexes bearing 3,5-di-*tert*-butylpyrazolato ligands (**2–6**, **8**, **9**) sublimed readily and quantitatively.

LANL2DZ level of theory as described in the Experimental Section. Figures 6 and 7 show the calculated geometrical parameters for **10** and **11**, respectively. If the center of the nitrogen–nitrogen bond of the η^2 -pyrazolato donor in **10** is considered to be a monodentate ligand, then the geometry of the computed structure can be regarded as distorted trigonal bipyramidal, similar to **2**. Like the pyridine ligands in **2**, the ammonia groups are in the axial positions. The computed yttrium–nitrogen bond lengths in **10** for the pyrazolato ligand (2.311, 2.312 Å) and for the ammine ligands (2.481, 2.482 Å) are very similar to the related values found in **2** (Y–N(pyrazolato), 2.323–2.405 Å; Y–N(pyridine), 2.503(3), 5.532(3) Å). The slightly longer bond lengths found in **2** probably reflect the larger steric crowding and less electrophilic metal center found in this molecule, compared to **10**. To provide a comparison with **10**, the pyrazolato ligand was constrained to be η^1 by fixing the yttrium–nitrogen–nitrogen angle at 126°. Optimization at the B3LYP/LANL2DZ level of theory yielded **11**, which was found to be 11.7 kcal/mol higher in energy than **10** at this level of theory. Adding polarization functions on yttrium and the pyrazolato nitrogen atoms lowers this value by only 0.2 kcal/mol. Closer inspection of **11** revealed a hydrogen

However, the 3,5-dimethylpyrazolato complex **7** decomposed upon attempted sublimation, indicating that the 3,5-dimethylpyrazolato ligand does not possess sufficient steric bulk to reduce the lattice energy to the point where sublimation is possible. The calculations also reveal that η^2 -pyrazolato ligand coordination is more stable than the η^1 -pyrazolato mode by about 20 kcal/mol. η^2 -Pyrazolato ligand coordination helps to saturate the coordination sphere, leading to electronically and sterically saturated metal centers. Therefore, η^2 -pyrazolato ligands may help to promote the formation of monomeric lanthanide complexes. Monomeric structures are essential to achieve the highest possible volatility for CVD applications. Alkyl substitution on the pyridine ligands did not affect the sublimation temperature for **2–4** and **8**, nor did substitution of pyridine by *n*-butylimidazole ligands in **6** or 3,5-di-*tert*-butylpyrazole in **9**. However, the *n*-butylimidazole complex **6** had a melting point that was nearly 100 °C lower than those of the analogous complexes containing pyridine-based ligands. We suggest that the long alkyl group affords a decreased melting point due to disruption of the crystal packing by accommodation of the groups projecting into the molecular void. Low melting source compounds are desirable, since the surface area of a liquid in a CVD bubbler remains approximately constant as the compound is being used. By contrast, the surface area of a solid changes as the amount of source compound in the bubbler decreases, leading to variable source compound concentrations in the gaseous precursor stream.

Lanthanide complexes bearing substituted 1,3-diketonate ligands are widely used as source compounds for the deposition of oxide materials.⁵⁵ In **2–9**, the η^2 -pyrazolato ligands bear a significant resemblance to 1,3-diketonate ligands, in that the ligand bears a negative charge, both nitrogen atoms of the pyrazolato ligand are coordinated to the metal, and the steric profile of the ligand can be controlled by appropriate substitution on the carbon atoms. As we have proposed previously in the context of magnesium⁴⁵ and titanium⁴⁶ pyrazolato complexes, we suggest that there is a strong analogy between complexes bearing η^2 -pyrazolato ligands and those containing 1,3-diketonate ligands. The present work demonstrates that the idea of exchanging pyrazolato ligands for diketonate ligands in the lanthanide elements leads to thermally stable, volatile complexes that can be used in CVD applications where source compounds bearing 1,3-diketonate ligands are inappropriate, i.e., erbium-doped group 13–15 semiconductor films.^{39–41} On the basis of our demonstration of the volatile yttrium, erbium, and lutetium complexes **2**, **4–6**, and **8**, we suggest that complexes of the formula $\text{Ln}(\text{3,5-tBu}_2\text{pz})_3(\text{N-donor})_2$ (N-donor = neutral aromatic nitrogen donor) will be volatile for all of the lanthanide elements, and should function as precursors in CVD processes.

Compounds used for the fabrication of semiconductor materials must meet exceptionally stringent purity standards to provide materials acceptable for device applications. Since we have used **4** extensively to prepare erbium-doped GaAs films, it was essential that we establish the concentration of elemental contaminants present in **4** at the part per million or greater level. A significant problem in this endeavor is that the purest grade of lanthanide metals that is commonly available is 99.9%, and this grade apparently refers only to other lanthanides. Our analysis of the erbium metal used to prepare **4** indeed revealed detectable amounts of 15 elements, including 7 lanthanide elements that totaled nearly 0.2% of the erbium content. Upon formation of **4** from the erbium metal, followed by purification

through two sublimations, the level of all element contaminants fell dramatically, and the total content of lanthanides other than erbium was about 0.02%. These analyses indicate that **4** can be obtained in a very high degree of purity through simple laboratory manipulations (e.g., sublimation). The high degree of purity, coupled with the lack of elements other than carbon, hydrogen, and nitrogen in the coordination sphere, indicates that **4** cannot introduce undesired elements into film deposition processes in which it is used.

We have reported that **4** can be used as the erbium source in a CVD process to produce erbium-doped GaAs epitaxial films, and that these films provide sharp luminescence (line width $<0.7 \text{ cm}^{-1}$) at 1540 nm resulting from the $^4\text{I}_{13/2} \rightarrow ^4\text{I}_{15/2}$ emission characteristic of the erbium(III) ion.^{39–41} Significantly, the luminescence of an erbium-doped GaAs film deposited using tris(*tert*-butylcyclopentadienyl)erbium as the erbium source gave films exhibiting a broad emission (40 cm^{-1}) at 1540 cm^{-1} , suggesting that the erbium is present in many different types of sites.³⁹ The concentration of the erbium ion in the GaAs film fabricated using **4** as the erbium source was found to be about 10^{16} cm^{-3} , which corresponds to about 1 ppm. Despite the low concentration of erbium, the luminescence from films derived from **4** was very strong due to the formation of a single efficient emissive site. Spectroscopic analysis of the films fabricated using **4** suggested that the luminescent erbium site consists of an erbium(III) ion sitting on a gallium site, surrounded by two oxygen and two arsenic atoms. This type of emissive erbium site, abbreviated as Er-2O, has been extensively investigated by Takahei.^{56–60} To produce the Er-2O center, Takahei employed cyclopentadienyl erbium sources and introduced a few parts per million of oxygen gas into the film growth chamber. In our depositions using **4**, no intentional oxygen source was added to the source flow. We suggest that the oxygen in the film arises from gettering of trace amounts of oxygen compounds in the reactor by erbium atoms present on the surface of the film, rather than from oxygen contamination in **4**. Exposure of **4** to water leads to instant elimination of 3,5-di-*tert*-butylpyrazole, along with presumed oligomeric erbium oxo complexes. Such oligomeric complexes would be much less volatile than **4**, and would not be transported into the CVD reactor. Because of the fact that **4** introduces the highly emissive Er-2O luminescence site very efficiently, our future work will examine the intentional formation of the Er-2O luminescent site by using an added oxygen source. Presumably, intentional oxygen codoping will lead to a much higher concentration of the Er-2O emissive defect in the films with a corresponding increase in the luminescence intensity. We are also examining new erbium source compounds that may be superior to **4** in the fabrication of erbium-doped semiconductor films.

Experimental Section

General Considerations. All reactions were performed under an inert atmosphere of argon using either glovebox or Schlenk line techniques. Toluene, tetrahydrofuran, and triethylamine were distilled from sodium. Pyridine, 4-*tert*-butylpyridine, and *n*-butylimidazole were distilled from calcium hydride. Erbium and yttrium metal powders (40 mesh) were purchased from Strem Chemicals, Inc. 3,5-Dimethylpyra-

(55) For a review, see: Lewkebandara, T. S.; Winter, C. H. *Chemtracts Inorg. Chem.* **1994**, 6, 271.

(56) Takahei, K.; Taguchi, A.; Horikoshi, Y.; Nakata, J. *J. Appl. Phys.* **1994**, 76, 4332.

(57) Haase, D.; Dörnen, A.; Takahei, K.; Taguchi, A. *Mater. Res. Soc. Symp. Proc.* **1996**, 422, 179.

(58) Hogg, R. A.; Takahei, K.; Taguchi, A.; Horikoshi, Y. *Mater. Res. Soc. Symp. Proc.* **1996**, 422, 167.

(59) Takahei, K.; Taguchi, A. *J. Appl. Phys.* **1995**, 77, 1735; 78, 5614.

(60) Nakagome, H.; Uwai, K.; Takahei, K. *Appl. Phys. Lett.* **1988**, 53, 1726.

zole was obtained from Aldrich Chemical Co. Tris(cyclopentadienyl)erbium(III),⁶¹ tris(cyclopentadienyl)lutetium(III),⁶² tris(3,5-di-*tert*-butylpyrazolato)bis(tetrahydrofuran)yttrium(III) (**1**),³⁴ 3,5-di-*tert*-butylpyrazole,⁶³ and bis(pentafluorophenyl)mercury⁶⁴ were synthesized according to literature methods.

¹H and ¹³C{¹H} NMR were obtained at 300 or 75 MHz in benzene-*d*₆. Infrared spectra were obtained using Nujol as the medium. Elemental analyses were performed by Midwest Microlab, Indianapolis, IN. Melting points were obtained on a Haake-Buchler HBI digital melting point apparatus and are uncorrected.

Preparation of Tris(3,5-di-*tert*-butylpyrazolato)bis(pyridine)yttrium(III) (2). A 200-mL Schlenk flask was charged with yttrium metal (0.329 g, 3.70 mmol), bis(pentafluorophenyl)mercury (1.39 g, 2.60 mmol), 3,5-di-*tert*-butylpyrazole (0.936 g, 5.20 mmol), pyridine (0.276 g, 3.50 mmol), and toluene (50 mL). The resultant mixture was stirred at ambient temperature for 120 h, during which time a fine black precipitate was formed. After filtration through a 2-cm pad of Celite on a coarse glass frit, the volatile components were removed under reduced pressure to afford a colorless, microcrystalline solid. Sublimation of this crude material at 150 °C (0.1 mmHg) yielded colorless crystals of **2** (0.455 g, 33%): mp 249–251 °C; IR (Nujol, cm⁻¹) 3040 (w), 1601 (s), 1506 (s), 1487 (m), 1444 (vs), 1414 (m), 1359 (vs), 1316 (m), 1251 (s), 1222 (s), 1152 (m), 1069 (m), 1038 (s), 1018 (s), 997 (s), 792 (s), 758 (m), 700 (s), 626 (m); ¹H NMR (benzene-*d*₆, 23 °C, δ) 7.43 (m, 4 H, Py CH), 6.71 (m, 2 H Py CH), 6.42 (m, 3H, pyrazolato ring CH), 6.38 (m, 4 H, Py CH), 1.29 (s, 54 H, C(CH₃)₃); ¹³C{¹H} NMR (benzene-*d*₆, 23 °C, ppm) 159.29 (s, pyrazolato ring CC(CH₃)₃), 150.28 (s, Py CH), 137.67 (s, Py CH), 123.74 (s, Py CH), 101.68 (s, pyrazolato ring CH), 32.25 (s, pyrazolato C(CH₃)₃), 31.49 (s, pyrazolato C(CH₃)₃). Anal. Calcd for C₄₃H₆₇N₈Y: C, 65.80; H, 8.60; N, 14.27. Found: C, 66.10; H, 8.79; N, 14.45.

Preparation of Tris(3,5-di-*tert*-butylpyrazolato)yttrium(III) (3). Complex **1** (0.502 g, 0.652 mmol) was heated in a horizontal tube furnace at 180–190 °C (0.1 mmHg) for 18 h. Compound **3** sublimed as a white solid (0.155 g, 38%): mp 230–240 °C dec; IR (Nujol, cm⁻¹) 1555 (m), 1522 (m), 1503 (s), 1412 (m), 1360 (vs), 1250 (vs), 1226 (m), 1020 (s), 997 (s), 805 (m), 796 (s); ¹H NMR (benzene-*d*₆, 23 °C, δ) 6.16 (s, 3 H, pz ring CH), 1.24 (s, 54 H, C(CH₃)₃); ¹³C{¹H} NMR (benzene-*d*₆, 23 °C, ppm) 160.44 (s, ring CC(CH₃)₃), 101.51 (s, ring CH), 32.14 (s, ring C(CH₃)₃), 30.93 (s, C(CH₃)₃). Anal. Calcd for C₃₃H₅₇N₈Y: C, 63.24; H, 9.17; N, 13.41. Found: C, 62.67; H, 8.92; N, 13.29.

Preparation of Tris(3,5-di-*tert*-butylpyrazolato)bis(4-*tert*-butylpyridine)erbium(III) (4). In a fashion similar to the preparation of **2**, erbium metal (3.09 g, 18.5 mmol), bis(pentafluorophenyl)mercury (6.95 g, 13.0 mmol), 3,5-di-*tert*-butylpyrazole (4.68 g, 26.0 mmol), 4-*tert*-butylpyridine (2.36 g, 17.5 mmol), and toluene (100 mL) were reacted to afford pink crystals of **4** (5.30 g, 63%): mp 241–243 °C; IR (Nujol, cm⁻¹) 1608 (s), 1498 (m), 1355 (s), 1259 (vs), 1226 (m), 1087 (s), 1016 (vs), 791 (vs). Crystals suitable for single-crystal X-ray diffraction were grown by sublimation at 150 °C (0.1 mmHg). Anal. Calcd for C₅₁H₈₃ErN₈: C, 62.81; H, 8.51; N, 11.49. Found: C, 62.73; H, 8.47; N, 11.52.

Complex **4** was also prepared from tris(cyclopentadienyl)erbium(III): A 200-mL Schlenk flask was charged with tris(cyclopentadienyl)erbium(III) (0.500 g, 1.38 mmol), 4-*tert*-butylpyridine (0.378 g, 2.80 mmol), and toluene (50 mL). After 0.5 h of stirring at ambient temperature, all solids dissolved and the resultant solution was added by a cannula to a solution of 3,5-di-*tert*-butylpyrazole (0.744 g, 4.13 mmol) in toluene (20 mL). The resultant mixture was stirred for 24 h at ambient temperature. The volatile components were removed under reduced pressure to afford a pink microcrystalline solid, which was sublimed at 150 °C (0.1 mmHg) to yield pink crystals of **4** (0.551 g, 41%): mp 242–244 °C. Anal. Calcd for C₅₁H₈₃ErN₈: C, 62.81; H, 8.51; N, 11.49. Found: C, 62.53; H, 8.54; N, 11.63.

Preparation of Tris(3,5-di-*tert*-butylpyrazolato)bis(pyridine)erbium(III) (5). In a fashion similar to the preparation of **2**, erbium metal (0.619 g, 3.70 mmol), bis(pentafluorophenyl)mercury (1.39 g, 2.60 mmol), 3,5-di-*tert*-butylpyrazole (0.936 g, 5.20 mmol), pyridine (0.276 g, 3.50 mmol), and toluene (50 mL) were reacted to afford **5** as pink crystals (1.32 g, 88%): mp 252–254 °C; IR (Nujol, cm⁻¹) 1598 (s), 1508 (s), 1412 (m), 1360 (vs), 1312 (m), 1250 (s), 1221 (m), 1035 (m), 1016 (s), 992 (m), 791 (s), 696 (m). Anal. Calcd for C₄₃H₆₇ErN₈: C, 59.82; H, 7.82; N, 12.98. Found: C, 59.81; H, 7.99; N, 12.93.

Preparation of Tris(3,5-di-*tert*-butylpyrazolato)bis(*n*-butylimidazole)erbium(III) (6). In a fashion similar to the preparation of **2**, erbium metal (0.619 g, 3.70 mmol), bis(pentafluorophenyl)mercury (1.39 g, 2.60 mmol), 3,5-di-*tert*-butylpyrazole (0.936 g, 5.20 mmol), *n*-butylimidazole (0.600 g, 4.84 mmol), and toluene (50 mL) were reacted to afford **6** as pink crystals suitable for X-ray crystallography (0.793 g, 48%): mp 163–168 °C; IR (Nujol, cm⁻¹) 3105 (m), 1517 (vs), 1498 (vs), 1407 (m), 1355 (vs), 1317 (m), 1250 (s), 1226 (s), 1202 (m), 1106 (s), 1092 (m), 1016 (m), 992 (s), 934 (s), 829 (m), 777 (vs), 748 (m), 657 (m). Anal. Calcd for C₄₇H₈₁ErN₈: C, 59.21; H, 8.56; N, 14.69. Found: C, 59.22; H, 8.89; N, 14.56.

Preparation of Tris(3,5-dimethylpyrazolato)bis(4-*tert*-butylpyridine)erbium(III) (7). In a fashion similar to the preparation of **2**, erbium metal (0.619 g, 3.70 mmol), bis(pentafluorophenyl)mercury (1.39 g, 2.60 mmol), 3,5-dimethylpyrazole (0.499 g, 5.20 mmol), and 4-*tert*-butylpyridine (0.468 g, 3.50 mmol) were reacted in toluene (50 mL). The volatile components were removed under reduced pressure to afford a pink, sticky solid. This solid was extracted with toluene (40 mL), and the resultant mixture was filtered through a 2-cm pad of Celite on a coarse glass frit. The resultant clear, pink solution was concentrated to a volume of ca. 30 mL and then stored at –20 °C for 24 h to afford pink crystals of **7** (0.628 g, 50%): mp 140–150 °C dec; IR (Nujol, cm⁻¹) 1603 (s), 1512 (s), 1259 (m), 1226 (m), 1006 (s), 829 (m), 791 (m), 777 (s). Anal. Calcd for C₃₃H₄₇ErN₈: C, 54.83; H, 6.51; N, 15.16. Found: C, 54.19; H, 6.20; N, 15.57.

Preparation of Tris(3,5-di-*tert*-butylpyrazolato)bis(4-*tert*-butylpyridine)lutetium(III) (8). In a fashion similar to the preparation of **4** from tris(cyclopentadienyl)erbium(III), tris(cyclopentadienyl)lutetium(III) (0.250 g, 0.676 mmol), 3,5-di-*tert*-butylpyrazole (0.364 g, 2.03 mmol), and 4-*tert*-butylpyridine (0.183 g, 1.35 mmol) were reacted to afford colorless crystals of **8** (0.551 g, 83%): mp 233–236 °C; IR (Nujol, cm⁻¹) 1608 (vs), 1541 (m), 1503 (vs), 1431 (s), 1412 (s), 1355 (vs), 1312 (m), 1250 (vs), 1226 (s), 1202 (m), 1068 (m), 1016 (vs), 992 (s), 829 (s), 786 (vs); ¹H NMR (benzene-*d*₆, 23 °C, δ) 7.39 (m, 4 H, 4-*tert*-butylpyridine ring CH), 6.63 (m, 4 H, 4-*tert*-butylpyridine ring CH), 6.58 (s, 3 H, pyrazolato ring CH), 1.32 (s, 54 H, pyrazolato C(CH₃)₃), 0.77 (s, 18 H, 4-*tert*-butylpyridine C(CH₃)₃); ¹³C{¹H} NMR (benzene-*d*₆, 23 °C, ppm) 162.13 (s, 4-*tert*-butylpyridine ring CH), 158.97 (s, pyrazolato ring CC(CH₃)₃), 150.44 (s, 4-*tert*-butylpyridine ring CH), 120.91 (s, 4-*tert*-butylpyridine ring CH), 101.90 (s, pyrazolato ring CH), 34.50 (s, 4-*tert*-butylpyridine C(CH₃)₃), 32.27 (s, pyrazolato ring C(CH₃)₃), 31.55 (s, pyrazolato C(CH₃)₃), 29.91 (s, 4-*tert*-butylpyridine C(CH₃)₃). Anal. Calcd for C₅₁H₈₃LuN₈: C, 62.30; H, 8.51; N, 11.40. Found: C, 61.91; H, 8.55; N, 11.44.

Preparation of Tris(3,5-di-*tert*-butylpyrazolato)(3,5-di-*tert*-butylpyrazole)erbium(III) (9). In a fashion similar to the preparation of **2**, erbium metal (0.619 g, 3.70 mmol), bis(pentafluorophenyl)mercury (1.39 g, 2.60 mmol), 3,5-di-*tert*-butylpyrazole (1.404 g, 7.80 mmol), triethylamine (0.500 g, 4.95 mmol), and toluene (50 mL) were reacted to afford **9** as pink crystals (1.01 g, 59%): mp 272–274 °C; IR (Nujol, cm⁻¹) 3286 (m, broad, ν_{NH}), 1556 (m), 1523 (s), 1504 (vs), 1416 (m), 1359 (vs), 1312 (m), 1251 (m), 1227 (s), 1018 (s), 991 (s), 806 (m), 792 (s). Anal. Calcd for C₄₄H₇₇ErN₈: C, 59.69; H, 8.77; N, 12.66. Found: C, 59.73; H, 8.85; N, 12.75.

Elemental Analysis of Erbium Metal and 4 by Inductively Coupled Plasma Optical Emission Spectroscopy. Approximately 0.1 g of each sample was accurately weighed and dissolved in concentrated nitric acid (2.00 mL). This solution was then diluted to 100.0 mL in a volumetric flask using distilled water. Stock standard solutions of 0.00, 0.05, 0.10, 0.15, and 0.20 ppm of various mixtures of the standard solutions were prepared. A 0.50-mL sample of each solution was added to the “unknown” samples of erbium metal or **4** using the standard

(61) Wilkinson, G.; Birmingham, J. M. *J. Am. Chem. Soc.* **1955**, *78*, 42.

(62) Fischer, E. O.; Fiescher, H. *J. Organomet. Chem.* **1965**, *3*, 181.

(63) Elguero, J.; Gozalez, E.; Jacquier, R. *Bull. Soc. Chim. Fr.* **1968**, 707.

(64) Albrecht, H. B.; Deacon, G. B.; Tailby, M. J. *J. Organomet. Chem.* **1974**, *70*, 313.

addition method. For determination of the elemental composition of **4**, a 2.00-mL aliquot of the dissolved complex was added to each flask.

The analyses were performed on a Perkin-Elmer Optima model 3000 inductively coupled plasma spectrometer. The forward power was 1.2 kW. The support gas was argon, with a plasma flow rate of 1.5 L/min, an auxiliary flow rate of 0.5 L/min, and a nebulizer flow rate of 0.8 L/min. The peristaltic pump was set at a flow rate of 1.0 L/min. The viewing height above the load coil was 15 mm. The nitric acid that was used to dissolve the samples was Ultrex II Ultrapure grade obtained from J. T. Baker, Phillipsburg, NJ. Water used in the analyses was doubly distilled and deionized. The elemental standards used to quantify the concentrations were manufactured and certified by High Purity Standards, Charleston, SC. A complete list of the results obtained for **4** and the erbium metal used to prepare **4** is given in the Supporting Information. "N.D." implies that an element was "not detected" under the given conditions. In such cases the number in parentheses is an estimation of the detection limit based on extrapolation of the calibration curve and assumption of a signal-to-noise ratio of 3/1.

Molecular Orbital Calculations. GAUSSIAN 98⁶⁵ was used to carry out electronic structure calculations employing hybrid density functional methods and pseudopotentials. Equilibrium geometries were optimized using redundant internal coordinates⁶⁶ and analytical gradients. A three-parameter density functional method (B3LYP^{67–69}) was used with the Los Alamos pseudopotentials and a double- ζ basis set (LANL2DZ^{70–72}): for yttrium this corresponds to two sets of 5s, 5p, and 4d functions, one set of 4s and 4p functions, and the remaining inner electrons replaced by pseudopotentials; for chlorine, two sets of 3s and 3p functions with the 1s, 2s, and 2p replaced by pseudopotentials; for hydrogen, carbon, and nitrogen, the D95V basis⁷³ without pseudopotentials. Additional single-point calculations were carried out with polarization functions on yttrium (a set of seven 4f Gaussians with exponent 0.19⁷⁴) and the pyrazolato nitrogens (a set of five 3d Gaussians with exponent 0.80). Charge distributions were analyzed by the natural bond orbital (NBO) method at the B3LYP/LANL2DZ level of theory.⁷⁵

Crystallographic Structural Determinations of 4, 7, and 9. Suitable crystals were selected and mounted in thin-walled, nitrogen-

flushed glass capillaries. The data were collected on a Siemens P4 diffractometer equipped with a SMART CCD detector.

The systematic absences in the diffraction data are consistent with the tetragonal space groups $P4_12_12$ and $P4_32_12$ for **7**, uniquely consistent with the orthorhombic space group $Pbca$ for **4**, and uniquely consistent with the monoclinic space group $P2_1/c$ for **9**. The structures were solved using direct methods, completed by subsequent difference Fourier syntheses, and refined by full-matrix least-squares procedures. Refinement of **7** in $P4_12_12$ showed this to be the correct absolute configuration of the molecule (Flack parameter $-0.007(11)$). Absorption corrections were not applied to **4**, **7**, and **9**, because there was less than 10% variation in the integrated ψ -scan intensity data. The molecule of **7** lies on a 2-fold rotation axis. The methyl carbon atoms of the *tert*-butyl groups on the pyrazolato ligands, C(23)–C(25) and C(27)–C(29) of **4**, and C(5)–C(7) and C(9)–C(11) of **4**, were disordered over two positions (70/30, 60/40, 50/50, and 50/50, respectively). All non-hydrogen atoms were refined with anisotropic displacement coefficients, and hydrogen atoms were treated as idealized contributions. All software and sources of the scattering factors are contained in the SHELXTL (5.03 and 5.10) program libraries.⁷⁶

Crystallographic Structural Determinations of 2 and 8. Suitable crystals were selected and mounted in thin-walled, nitrogen-flushed glass capillaries. The data were collected on a Bruker automated P4/CCD diffractometer equipped with monochromated Mo radiation. A hemisphere of data was collected for each sample at 5 (**8**) or 10 (**2**) s/frame. The data were integrated with the manufacturer's SMART and SAINT software, respectively. Cell constants were refined with SAINT. Absorption corrections were applied with Bruker's XPREP program (**8**) or Sheldrick's SADABS program (**2**). The structures were solved and refined using the programs of SHELXS-86 and SHELXL-93.⁷⁶

For **2**, 24 351 total data were averaged to yield 9867 ($R_{\text{int}} = 0.039$) independent reflections. The compound crystallizes as a discrete molecular complex with no associated solvent or ions. Hydrogen atoms were calculated and assigned to ride on the carbon atom. Crystallographic parameters are given in Table 1. Some disorder is observed in the *tert*-butyl groups.

For **8**, 47 411 total data were averaged to yield 11 576 ($R_{\text{int}} = 0.075$) independent reflections. The compound crystallizes as a discrete molecular complex with no associated solvent or ions. All atoms occupy general positions in the cell. Hydrogen atoms were calculated and assigned to ride on the carbon atom. Crystallographic parameters are given in Table 1. The *tert*-butyl groups display large thermal parameters typical of disorder for these groups.

Acknowledgment. C.H.W. acknowledges support from the Army Research Office (J. Prater). T.F.K. acknowledges the support of the Army Research Office (J. Prater) and facilities support through the NSF-funded Materials Research Science and Engineering Center on Nanostructured Materials and Interfaces. H.B.S. acknowledges support from the National Science Foundation (Grant No. CHE-9874005).

Supporting Information Available: Tables listing the elements that were screened in the ICP-OES analyses, elemental composition of **4**, and the starting erbium metal determined by ICP-OES, as well as positional parameters for the calculated structures of **10** and **11**. X-ray crystallographic files in CIF format for the structure determination of **2** and **4–9**. This material is available free of charge via the Internet at <http://pubs.acs.org>.

IC9903190

- (65) Frisch, M. J.; Trucks, G. W.; Schlegel, H. B.; Scuseria, G. E.; Robb, M. A.; Cheeseman, J. R.; Zakrzewski, V. G.; Montgomery, J. A.; Stratmann, R. E.; Burant, J. C.; Dapprich, S.; Millam, J. M.; Daniels, A. D.; Kudin, K. N.; Strain, M. C.; Farkas, O.; Tomasi, J.; Barone, V.; Cossi, M.; Cammi, R.; Mennucci, B.; Pomelli, C.; Adamo, C.; Clifford, S.; Ochterski, J.; Petersson, G. A.; Ayala, P. Y.; Cui, Q.; Morokuma, K.; Malick, D. K.; Rabuck, A. D.; Raghavachari, K.; Foresman, J. B.; Cioslowki, J.; Ortiz, J. V.; Stefanov, B. B.; Liu, G.; Liashenko, A.; Piskorz, P.; Komaromi, I.; Gomperts, R.; Martin, R. L.; Fox, D. J.; Keith, T.; Al-Laham, M. A.; Peng, C. Y.; Nanayakkara, A.; Gonzalez, C.; Challacombe, M.; Gill, P. M. W.; Johnson, B. G.; Chen, W.; Wong, M. W.; Andres, J.; Head-Gordon, M.; Replogle, E. S.; Pople, J. A. *GAUSSIAN 98*; Gaussian, Inc.: Pittsburgh, PA, 1998.
- (66) Peng, C.; Ayala, P. Y.; Schlegel, H. B.; Frisch, M. J. *J. Comput. Chem.* **1996**, *17*, 49.
- (67) Becke, A. D. *Phys. Rev. A* **1988**, *38*, 3098.
- (68) Lee, C.; Yang, W.; Parr, R. D. *Phys. Rev. B* **1988**, *37*, 785.
- (69) Becke, A. D. *J. Chem. Phys.* **1993**, *98*, 5648.
- (70) Hay, P. J.; Wadt, W. R. *J. Chem. Phys.* **1985**, *82*, 270.
- (71) Wadt, W. R.; Hay, P. J. *J. Chem. Phys.* **1985**, *82*, 284.
- (72) Hay, P. J.; Wadt, W. R. *J. Chem. Phys.* **1985**, *82*, 299.
- (73) Dunning, T. H., Jr.; Hay, P. J. In *Modern Theoretical Chemistry*; Schaefer, H. F., Ed.; Plenum: New York, 1976; p 1.
- (74) Walch, S. P.; Bauschlicher, C. W., Jr.; Nelin, C. J. *J. Chem. Phys.* **1983**, *79*, 3600.
- (75) Reed, A. E.; Weinhold, F. *J. Chem. Phys.* **1983**, *78*, 4066.
- (76) Sheldrick, G., Institut für Anorg. Chemie, Tammannstrasse 4, D-37077 Göttingen, Germany.